

See discussions, stats, and author profiles for this publication at: <https://www.researchgate.net/publication/267811806>

Mott Transition in a Two Leg Bose Hubbard Ladder Under an Artificial Magnetic Field

ARTICLE *in* PHYSICAL REVIEW A · NOVEMBER 2014

Impact Factor: 2.81 · DOI: 10.1103/PhysRevA.91.013629 · Source: arXiv

CITATIONS

2

READS

24

2 AUTHORS, INCLUDING:



M. O. Oktel

Bilkent University

46 PUBLICATIONS 517 CITATIONS

SEE PROFILE

Mott Transition in a Two Leg Bose Hubbard Ladder Under an Artificial Magnetic Field

Ahmet Keleş^{1,2,*} and M. Ö. Oktel^{3,†}

¹*Department of Physics and Astronomy, University of Pittsburgh, Pittsburgh, PA 15260*

²*School of Physics and Astronomy and Computational Sciences, George Mason University, Fairfax, VA 15260*

³*Department of Physics, Bilkent University, 06800, Ankara, TURKEY*

We consider the Bose Hubbard model on a two leg ladder under an artificial magnetic field, and investigate the superfluid to Mott insulator transition in this setting. Recently, this system has been experimentally realized [M. Atala et al., *Nature Physics* 10, 588-593 (2014)], albeit in a parameter regime that is far from the Mott transition boundary. Depending on the strength of the magnetic field, the single particle spectrum has either a single ground state or two degenerate ground states. The transition between these two phases is reflected in the many particle properties. We first investigate these phases through the Bogoliubov approximation in the superfluid regime and calculate the transition boundary for weak interactions. For stronger interactions the system is expected to form a Mott insulator. We calculate the Mott transition boundary as a function of magnetic field and inter-leg coupling with mean field theory, strong coupling expansion and density matrix renormalization group (DMRG). Finally, using DMRG, we investigate the particle-hole excitation gaps of this system at different filling factors and find peaks at simple fractions indicating the possibility of correlated phases.

PACS numbers: 05.30.Jp, 05.70.Fh, 67.25.dj, 03.75.Lm, 73.43.-f, 05.10.-a

I. INTRODUCTION

Cold atom experiments can realize fundamental models of many particle physics which are not accessible with traditional condensed matter techniques. One recent advance has been the demonstration of artificial magnetic fields in optical lattice systems, as well as in continuum [1–3]. The optical lattice experiments control the phase of the hopping between different lattice sites to create a Hamiltonian with an artificial magnetic field. This effective magnetic field is orders of magnitude larger than what is attainable in a solid state experiment. For the typical lattice constants in solids, the magnetic flux through a unit cell is comparable to flux quantum h/e only for magnetic fields in excess of thousands of Tesla. The first experiments demonstrating effective magnetic fields in the optical lattices have proved that this extremely high magnetic field regime is accessible with cold atoms [2, 3].

Most investigations of the magnetic field effects on many particle systems rely on a separation of length scales, assuming that the magnetic length is much larger than the lattice scale. However, if these two length scales are comparable, the magnetic field can no longer be treated semiclassically and has to be directly taken into account in the microscopic Hamiltonian. The profound effect of such strong magnetic fields can be observed even for non-interacting particles. The single particle spectrum is sensitively dependent on the external field, forming a self-similar structure known as the Hofstadter butterfly [4]. The recent experiments hold the promise for investigation of many-particle physics for systems with such complicated single particle dispersion. The interplay between interactions and the complicated single particle spectrum is expected to result in novel phases [5, 6].

The first experiments which implemented an artificial magnetic field for lattice systems demonstrated the existence of the

artificial magnetic field by measuring the effect of this field on excited states of the system [7]. Thus they have not probed the ground state of the Hofstadter-Hubbard Hamiltonian. The recent experiment by the Munich group have for the first time demonstrated the effects of the artificial magnetic field on the ground state of a lattice system.

The experiment in Ref. [7] realizes a model which is essentially one dimensional. In general, the orbital coupling of the magnetic field to a one dimensional system does not create any change, as such a field can be set to zero by a gauge transformation. However, by using a two leg ladder, the experiment creates a situation for which the magnetic field has non-trivial effects on the system without generating a complicated single particle spectrum or a sensitive dependence on the rationality of the applied field. Thus, experimental realization of this system provides the first opportunity to study the behavior of lattice bosons in the extremely high magnetic field regime.

In this paper, we investigate this model system theoretically, particularly focusing on the effect of the artificial magnetic field on the Mott insulator to superfluid transition. We have previously conducted a theoretical study of the two leg Bose-Hubbard ladder [8]. In this paper our unpublished results are summarized and extended to cover the regime investigated by the experiment. The paper is organized as follows: We introduce the Hamiltonian in section (II), and review the properties of the single particle spectrum in section (III). In section (IV), we investigate the system with weak interactions using the Gross-Pitaevskii mean field approximation and also discuss the excitations of the system above the mean field solution. The remaining sections focus on the strongly interacting regime. In section (V), we calculate the phase diagram of the system using a real space Gutzwiller ansatz. This approximation is particularly poor for one dimensional systems, thus in section (VI) we calculate the phase diagram using strong coupling perturbation theory. Section (VII) contains the discussion of the Mott transition using DMRG. In section (VIII), we investigate the gap between the ground and the first excited

* ahmetkeles99@gmail.com

† oktel@fen.bilkent.edu.tr

state of the system at half filling in the infinite interaction limit as well as the gaps in the particle hole excitations of the system for various fillings using DMRG and discuss the possibility of correlated states. Finally, we summarize our results and their consequences for experiments in section (IX).

II. MODEL

We consider an infinite ladder composed of square plaquettes extending in the \hat{x} direction, with nearest neighbor hopping. The tight-binding Hamiltonian for this two leg ladder is given by

$$H = - \sum_i \left[J e^{-i\alpha} a_i^\dagger a_{i+1} + J e^{i\alpha} b_i^\dagger b_{i+1} + K a_i^\dagger b_i + H.C. \right] + \frac{U}{2} \sum_i n_i^a (n_i^a - 1) + n_i^b (n_i^b - 1) - \mu \sum_i n_i^a + n_i^b \quad (1)$$

where a_i, b_i (a_i^\dagger, b_i^\dagger) are bosonic annihilation (creation) operators for the i^{th} site in the upper and lower legs, respectively. $n_i^a = a_i^\dagger a_i$ and $n_i^b = b_i^\dagger b_i$ are corresponding number operators, J (K) is the intra-leg (inter-leg) hopping strength, U is the on-site interaction strength and μ is the chemical potential. We assume a homogeneous system that has “up-down” symmetry for zero magnetic field, so that on-site interactions and chemical potentials are identical for each leg. The phase α accumulated by hopping from \vec{r}_i to \vec{r}_j is

$$\alpha = \frac{e}{\hbar} \int_{\vec{r}_i}^{\vec{r}_j} d\mathbf{r} \cdot \mathbf{A}(\mathbf{r}), \quad (2)$$

where \mathbf{A} is the vector potential satisfying $\nabla \times \mathbf{A} = \mathbf{B}$ and \mathbf{B} is the magnetic field perpendicular to the two leg plane. We use the Landau gauge $\mathbf{A} = -B y \hat{x}$ for $\mathbf{B} = B \hat{z}$, and choose $y = 0$ to be at the center of two legs so that upper and lower legs will be at position $y = c/2$ and $y = -c/2$, respectively. Thus, the exponent in Eq. (1) can be calculated from Eq. (2) as $\alpha = \pi \phi / \phi_0$ where ϕ is the magnetic flux passing through each plaquette and $\phi_0 = h/e$ is the flux quantum.

The main advantage of considering a two leg ladder as opposed to the two dimensional extended system is immediately obvious. For two dimensional systems, periodicity under translations can only be obtained when ϕ / ϕ_0 is taken to be a rational number p/q . Only then the symmetry broken by the specific gauge choice can be restored in a q -fold enlarged unit cell. The two leg ladder system does not require such a constraint so that calculations can be carried out for any real number α / π between zero and one. As such, the two leg system presents an opportunity to observe the non-trivial effects of an external field in a lattice system refrained from the added theoretical complication. The profound effect of the magnetic field is evident even in the single particle level which is presented in the next section.

III. SINGLE PARTICLE SOLUTION

We first give solutions for non-interacting particles; $U = 0$. Using the translational invariance along the x -direction, the

Fourier components of the field operators can be written as,

$$a_j = \frac{1}{\sqrt{L}} \sum_k a_k e^{ikj}, b_j = \frac{1}{\sqrt{L}} \sum_k b_k e^{ikj} \quad (3)$$

where the Fourier components satisfy the commutation $[a_k, a_{k'}^\dagger] = \delta_{kk'}$ and $[b_k, b_{k'}^\dagger] = \delta_{kk'}$, all other commutators being zero. For simplicity, we have taken $c = 1$ above so that all lengths are measured in units of the lattice constant. Using these transformations in Eq.(1), the following Hamiltonian can be obtained in the momentum space

$$H_{sp} = - \sum_k \left[\xi_{ak} a_k^\dagger a_k + \xi_{bk} b_k^\dagger b_k + K a_k^\dagger b_k + K b_k^\dagger a_k \right], \quad (4)$$

where ξ_{ak} and ξ_{bk} are $2J \cos(k - \alpha)$ and $2J \cos(k + \alpha)$, respectively. Diagonalization is achieved by the Bogoliubov transformation $A_k = \cos \theta a_k + \sin \theta b_k$, $B_k = -\sin \theta a_k + \cos \theta b_k$ where $\theta = \frac{1}{2} \arctan(\frac{2K}{\xi_{ak} - \xi_{bk}})$. The energy eigenvalues $\epsilon_{1,2}$ can be found as

$$\epsilon_{1,2} = -2 \cos(k) \cos(\alpha) \mp \sqrt{\tilde{K}^2 + 4 \sin^2 k \sin^2 \alpha}, \quad (5)$$

where $\tilde{K} = K/J$ and we normalize the energy with the inter-leg hopping J . In Fig. (1), we show the dispersion relation in the first Brillouin zone, for zero and non-zero magnetic fields. It can be seen that, as the strength of the field increases, band minimum in the dispersion shifts from $k = 0$ to two nonzero k values that are degenerate and symmetric around the origin. The critical field for this bifurcation depends on the parameter \tilde{K} as

$$\alpha_c = \cos^{-1} \left(-\frac{\tilde{K}}{4} \pm \sqrt{\frac{\tilde{K}^2}{16} + 1} \right). \quad (6)$$

Above this critical field, the ground state of the system will no longer be a spatially uniform state, but will be a superposition of the plane waves corresponding to the two minima that can be found from the dispersion as:

$$k_{min} = \pm \sin^{-1} \sqrt{\sin^2 \alpha - \frac{\tilde{K}^2}{4 \tan^2 \alpha}}. \quad (7)$$

In the Munich experiment [7], these two ground states were observed for weakly interacting bosons and have been named as the Meissner and Vortex phases, respectively.

As one can see from the Fig. (1), for small values of the magnetic field, there is no gap between the lower band and the upper band, whereas for the one $\alpha / \pi = 0.5$ there is a finite band gap between these two and it decreases as K/J reduced. We observe that this gap closes as $K/J \rightarrow 0$ and a singular point emerges at $k = 0$ in this limit. To show a more detailed behavior of the band gap, we plot the minimum and the maximum of the two bands as a function of the magnetic field for $K = J$ in Fig. (2). This plot can be regarded as the “Hofstadter butterfly” of the two leg ladder system. We see that a diamond shaped gapped region starts at $\alpha / \pi = 1/3$, takes its maximum value $2J$ at $\alpha / \pi = 1/2$ and closes at $\alpha / \pi = 2/3$. In Fig. (2), we also provide the value of the reciprocal lattice vector k_{min} as given in Eq. (7) at the band minimum as a function of magnetic field and the parameter K/J which is in agreement with [7].

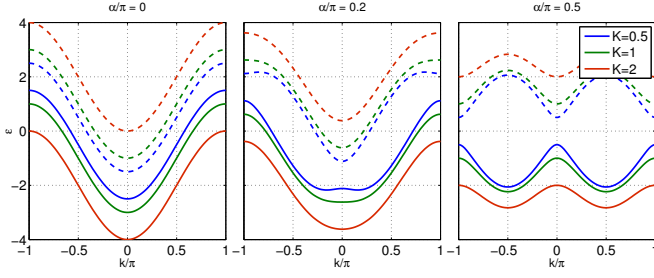


FIG. 1. Single particle spectrum of the two leg ladder with varying magnetic field α and inter-leg to intra-leg hopping ratio K (in units of J). Lower bands are shown with solid lines whereas upper bands are shown with dashed lines. The gap between lower and higher bands appears for $\alpha/\pi = 0.5$ is further shown below for the case $K = 1$ as a function of magnetic field in Fig.(2). It is also observed that gap around $k = 0$ for $\alpha/\pi = 0.5$ closes for very small $K \ll 1$ giving rise to a linear dispersion around $k = 0$.

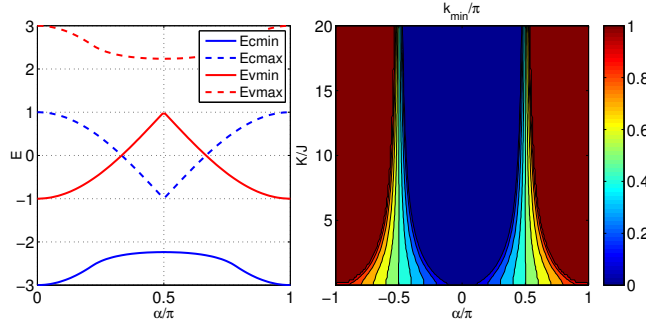


FIG. 2. (Left) Band minima and maxima for the two bands as a function of the magnetic field. Blue lines are for the lower band and red lines are for the higher band. Band minima are shown with solid lines, band maxima are shown with dashed lines. Band gap is evident in between $\alpha/\pi = 1/3$ and $\alpha/\pi = 2/3$ which attains its maximum value for $\alpha/\pi = 1/2$. (Right) Value of reciprocal lattice vector at the minimum energy as a function of magnetic field and parameter K/J .

IV. GROSS-PITAEVSKII APPROXIMATION

For small values of the interaction strength and the magnetic field, the system will essentially be in the superfluid state, mostly dominated by the hopping term in the Hamiltonian. Thus, assuming that the condensate fluctuations are negligible, we make the following approximation:

$$a_i \rightarrow \langle a_i \rangle = \psi_i, \quad b_i \rightarrow \langle b_i \rangle = \phi_i. \quad (8)$$

Both amplitude and the phase of those classical fields are time and position dependent. Clearly, approximation with a uniform condensate will fail above the critical field.

Making the substitution (8) in Eq. (1), the following energy functional is obtained (here we take $J = 1$ so that U , μ and K

are in the units of J);

$$E = - \sum_j [e^{-i\alpha} \psi_j^* \psi_{j+1} + e^{i\alpha} \phi_j^* \phi_{j+1} + K \psi_j^* \phi_j + c.c.] + \frac{U}{2} \sum_j [\psi_j^* \psi_j (\psi_j^* \psi_j - 1) + \phi_j^* \phi_j (\phi_j^* \phi_j - 1)] - \mu \sum_j |\psi_j|^2 + |\phi_j|^2. \quad (9)$$

Variation of the energy functional around the minimal solutions $i\partial \psi_i / \partial t = \delta E / \delta \psi_i^*$ and $i\partial \phi_i / \partial t = \delta E / \delta \phi_i^*$ gives the following coupled Gross-Pitaevskii equations:

$$i \frac{\partial \psi_j}{\partial t} = - [e^{-i\alpha} \psi_{j+1} + K \phi_j + e^{i\alpha} \psi_{j-1}] + U |\psi_j|^2 \psi_j - \left(\frac{U}{2} + \mu\right) \psi_j \quad (10)$$

$$i \frac{\partial \phi_j}{\partial t} = - [e^{i\alpha} \phi_{j+1} + K \psi_j + e^{-i\alpha} \phi_{j-1}] + U |\phi_j|^2 \phi_j - \left(\frac{U}{2} + \mu\right) \phi_j. \quad (11)$$

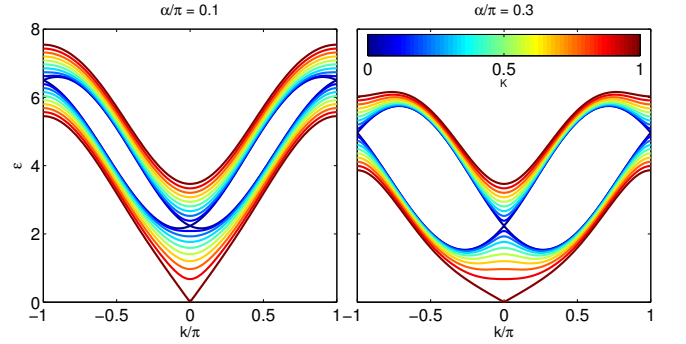


FIG. 3. Band diagrams for the two leg ladder with on-site interactions calculated within the Gross Pitaevskii approximation for $U = 2$. The left panel is for $\alpha/\pi = 0.1$ and the right panel is for $\alpha/\pi = 0.3$.

Zeroth order terms $\psi_j = \phi_j = \sqrt{n}$ give the chemical potential as $\mu = -(2 \cos \alpha + \tilde{K}) + 0.5U(2n - 1)$. For a higher order approximation, the fluctuations in the condensate is taken into account as[9]:

$$\psi_j = \sqrt{n} + A e^{i(kx_j - \omega t)} + B^* e^{-i(kx_j - \omega t)}, \quad \phi_j = \sqrt{n} + C e^{i(kx_j - \omega t)} + D^* e^{-i(kx_j - \omega t)}, \quad (12)$$

where A, B, C, D are small complex parameters, x_j is the position of the lattice site and k is the reciprocal lattice vector. Inserting these wave functions into Eq. (11), the equation of motion can be reduced to an algebraic equation of the form $H_{gp} \vec{\Psi} = \omega \vec{\Psi}$ where $\vec{\Psi} = (A, B, C, D)$ and H_{gp} has the form

$$H_{gp} = \begin{bmatrix} -\xi'_{ak} & Un & -K & 0 \\ -Un & \xi'_{bk} & 0 & K \\ -K & 0 & -\xi'_{bk} & Un \\ 0 & K & -Un & \xi'_{ak} \end{bmatrix}, \quad (13)$$

where $\xi'_{ak} = 2\cos(k - \alpha) - 2\cos(\alpha) - Un - K$ and $\xi'_{bk} = 2\cos(k + \alpha) - 2\cos(\alpha) - Un - K$. The resulting change in the spectrum can be obtained by calculating the eigenvalues of H_{gp} which is shown in Fig. (3).

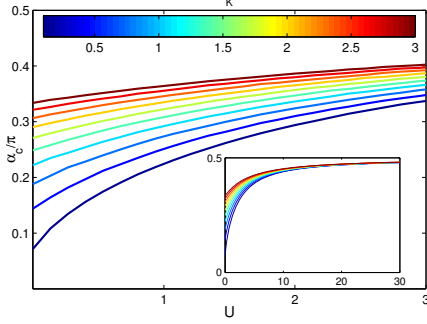


FIG. 4. Critical magnetic field plotted as a function of the interaction strength U and the intra-leg hopping K . Inset shows the same plot zoomed out for large interaction strengths. Note that the Gross-Pitaevskii approximation is not expected to be reliable for strong interactions.

Competition between the magnetic field and the interactions can be seen by considering the band minima around $k = 0$ in Fig. (3). Here the interactions sharpen the band and provide a cusp like shape whereas the increase of the magnetic field makes it smoother. The expansion of the wave function in Eq. (12) fails above the critical magnetic field, as the ground state is no longer spatially uniform. We have used this prop-

erty to determine the change of the critical field with the interaction strength. In Fig. (4), the critical magnetic field as function of the strength of the interaction is shown. It can be seen that, $U - \alpha_c$ relation is almost linear for small interaction strength but saturates for strong interactions. It must be noted that for strong interactions Gross Pitaevskii approximation is not reliable.

V. VARIATIONAL MEAN FIELD APPROACH

In this section, we consider the transition from the superfluid state to the Mott insulating state as a function of J , K , μ and α . Here, it is convenient to scale the Hamiltonian in Eq. (1) with $U = 1$. In the perfect Mott insulator phase, each site has a localized wave function with exactly n_0 particles such that the wave function in each site is $|n_0\rangle_i$ in the Fock basis. Allowing small variations around this equilibrium, we write the following Gutzwiller ansatz for local sites;

$$\begin{aligned} |G\rangle_{ak} &= \Delta_{ak}|n_0 - 1\rangle_{ak} + |n_0\rangle_{ak} + \Delta'_{ak}|n_0 + 1\rangle_{ak}, \\ |G\rangle_{bk} &= \Delta_{bk}|n_0 - 1\rangle_{bk} + |n_0\rangle_{bk} + \Delta'_{bk}|n_0 + 1\rangle_{bk}, \end{aligned} \quad (14)$$

where Δ and Δ' are small complex variational parameters. Wavefunction for a rung is $|G_r\rangle^k = |G\rangle_a^k |G\rangle_b^k$ so that the total wavefunction of the system can be written as $|\Psi\rangle = \prod_k |G\rangle_a^k |G\rangle_b^k$. Variational energy of the system is calculated from $\varepsilon = \langle \Psi | H | \Psi \rangle / \langle \Psi | \Psi \rangle$ up to second order in Δ and Δ' as follows:

$$\begin{aligned} \varepsilon = \sum_{i=1}^N \{ & -Je^{-i\alpha} [n_0\Delta_{a,i}\Delta_{a,i+1}^* + (n_0+1)\Delta_{a,i}'\Delta_{a,i+1}' + \sqrt{n_0(n_0+1)}\Delta_{a,i}\Delta_{a,i+1}' + \sqrt{n_0(n_0+1)}\Delta_{a,i}'\Delta_{a,i+1}^*] - Je^{i\alpha} [a \rightarrow b] \\ & - K [n_0\Delta_{a,i}\Delta_{b,i}^* + (n_0+1)\Delta_{a,i}'\Delta_{b,i}' + \sqrt{n_0(n_0+1)}(\Delta_{a,i}\Delta_{b,i}' + \Delta_{a,i}'\Delta_{b,i}^*)] \\ & + [(1-n_0+\mu)(|\Delta_{a,i}|^2 + |\Delta_{b,i}|^2) + n_0(n_0-1-2\mu) + (n_0-\mu)(|\Delta_{a,i}'|^2 + |\Delta_{b,i}'|^2)] \}. \end{aligned} \quad (15)$$

We minimize the energy with respect to Δ_{ai} , Δ_{bi} , Δ_{ai}' , Δ_{bi}' . The Jacobian matrix of the second derivatives are calculated as

$$\mathbf{J} = - \begin{pmatrix} n_0\mathbf{F} & \sqrt{n_0(n_0+1)}\mathbf{F} \\ \sqrt{n_0(n_0+1)}\mathbf{F} & (n_0+1)\mathbf{F} \end{pmatrix} + \begin{pmatrix} (1-n_0+\mu)\mathbf{I} & 0 \\ 0 & (n_0-\mu)\mathbf{I} \end{pmatrix}, \quad (16)$$

where \mathbf{I} is $2N \times 2N$ identity matrix and \mathbf{F} is written as

$$\mathbf{F} = \begin{bmatrix} A & B & \dots & B^\dagger \\ B^\dagger & A & \ddots & 0 \\ \vdots & \ddots & \ddots & B \\ B & 0 & B^\dagger & A \end{bmatrix}. \quad (17)$$

Here sub-blocks are defined in terms of Pauli matrices in the upper leg-lower leg basis as

$$A = K\sigma_x, \quad B = Je^{i\alpha\sigma_z}. \quad (18)$$

To find the eigenvalues, we use the same method presented in Ref.6; let $\lambda_{\mathbf{F}}$ and \vec{u} be the eigenvalues and the eigenvectors of \mathbf{F} respectively, then one can apply an ansatz of the form $\vec{v} = (a\vec{u}, b\vec{u})$ and solve the eigenvalue equation $\mathbf{J}\vec{v} = \lambda\vec{v}$ which is found to be

$$\lambda_{1,2} = 1 - \lambda_{\mathbf{F}}(2n_0+1) \pm \sqrt{(1 - \lambda_{\mathbf{F}}(2n_0+1))^2 + 4\lambda_{\mathbf{F}}(\mu+1) - 4(n_0-\mu)(1-n_0+\mu)} \quad (19)$$

Equating the minimum eigenvalue of the Jacobian matrix in Eq. (19) to zero yields the phase boundary of the Mott insulating region. Solving the corresponding equation for K and J , the following simple relation can be found for the boundary of Mott phase

$$\lambda_{\mathbf{F}}(K_c, J_c) = \frac{(n_0 - \mu)(1 - n_0 + \mu)}{(\mu + 1)}. \quad (20)$$

Here $\lambda_{\mathbf{F}}$ is the minimum value of ϵ_1 in Eq. 5 so that we obtain the Mott phase boundary for each value of the magnetic field α . In Fig. (5), Eq. (20) is plotted for $n_0 = 1$ which shows the shape of the Mott insulation region.

Note that this result is exact within the mean field theory. However, the mean field theory in a quasi one dimensional system is not expected to be accurate. The decoupling of the hopping term in Eq. 1 by introducing a mean field is questionable in a low dimensional system, where effect of fluctuations are necessarily important. The mean field calculation can only describe the system at a qualitative level. It provides a general idea about the topology of the Mott region, and an estimate of the phase boundary for small values of the hopping strength where site-site correlations are diminished. For a better determination the Mott insulating region, we turn to more accurate methods in the following sections.

VI. STRONG COUPLING EXPANSION

A better description of the transition is obtained by treating the hopping term as a perturbation on the perfect Mott state. While this is, in spirit, close to the mean field approach given in the previous section, correlations between the sites are built in as higher orders in perturbation theory are developed. The resulting ‘strong coupling expansion’ has been successfully applied to Bose-Hubbard model in low dimensions and has been shown to be in perfect agreement with accurate numerical methods [10, 11].

In strong coupling expansion, the hopping amplitude is considered as a small parameter. The Mott insulator state is characterized by a finite gap for particle-hole excitations, whereas this gap vanishes for the superfluid phase[12]. We calculate the energy of a system with exactly n_0 particles per site (Mott state E_M) and the energy of a system with one additional defect (particle E_P or hole E_H) perturbatively. The energy difference between the defect states and the perfect Mott state vanishes at the phase boundary. This method has been used for systems with different dimensions[13, 14] and for a two dimensional system under a magnetic field[15].

For the calculations in perturbation theory, it is convenient to write the Hamiltonian in the following generalized form:

$$H = - \sum_{ij} \mathbf{F}_{ij} a_i^\dagger a_j + \frac{1}{2} \sum_i n_i(n_i - 1) - \mu \sum_i n_i \quad (21)$$

where \mathbf{F} is given in Eq.(17) for our model.

We perform strong coupling perturbation up to second order in our calculations. The energies of the Mott state E_M , the

additional particle state E_P and the additional hole state E_H are found to be

$$E_M = E_M^0 - N n_0(n_0 + 1)(2J^2 + K^2), \quad (22)$$

$$E_P = E_P^0 - (n_0 + 1)\lambda_{\mathbf{F}} - N n_0(n_0 + 1)(2J^2 + K^2) - n_0(n_0 + 1)\lambda_{\mathbf{F}}^2 + \frac{1}{2} n_0(5n_0 + 4)(2J^2 + K^2), \quad (23)$$

$$E_H = E_H^0 - n_0\lambda_{\mathbf{F}} - N n_0(n_0 + 1)(2J^2 + K^2) - n_0(n_0 + 1)\lambda_{\mathbf{F}}^2 + \frac{1}{2} (n_0 + 1)(5n_0 + 1)(2J^2 + K^2), \quad (24)$$

where $\lambda_{\mathbf{F}}$ is the lowest eigenvalue of hopping matrix \mathbf{F} and N is the number of lattice sites in one leg. Zeroth order energies are $E_M^0 = 2N(n_0(n_0 - 1)/2 - \mu n_0)$, $E_P^0 = E_M^0 + n_0 - \mu$ and $E_H^0 = E_M^0 - (n_0 - 1) + \mu$. Solving the equations $E_P - E_M = 0$ and $E_M - E_H = 0$ for the chemical potential μ separately, the phase boundary of the particle sector and hole sector is obtained as,

$$\mu_P = n_0 + (n_0 + 1)\lambda_{\mathbf{F}} - n_0(n_0 + 1)\lambda_{\mathbf{F}}^2 + \frac{1}{2} n_0(5n_0 + 4)(2J^2 + K^2), \quad (25)$$

$$\mu_H = (n_0 - 1) - n_0\lambda_{\mathbf{F}} - n_0(n_0 + 1)\lambda_{\mathbf{F}}^2 - \frac{1}{2} (n_0 + 1)(5n_0 + 1)(2J^2 + K^2). \quad (26)$$

Here the magnetic field dependence comes indirectly from the eigenvalue $\lambda_{\mathbf{F}}$, but higher order terms in the perturbation will depend on the magnetic field explicitly. An interesting observation is that our results to this order are similar to the results of Ref. 15 for number of nearest neighbors equal to 3. However this is not guaranteed for higher order expansions since the flux attained through hopping is different due to difference of the topology of this constrained problem. Eigenvalue spectrum of the \mathbf{F} matrix is shown in Fig. (2).

In Fig. (6) we show the results of this calculation. An increase of the magnetic field enlarges the Mott insulating region of the phase diagram. This is expected as the magnetic field localizes the single particle trajectories even for the non-interacting problem thus a transition to an insulator state is easier. The Mott lobe grows in size until $\alpha = 0.5$ and then reduces to satisfy periodicity at $\alpha = 1$. The shape of the lobe is not concave as predicted by mean field, but convex with a cusp at the tip. This shape is generic in one dimension, as obtained by strong coupling, Monte Carlo and DMRG results in one dimension. By comparing Fig. (5) Fig. 6, it can be observed that the mean field results underestimate the Mott boundary by a considerable amount.

A new feature of the phase diagram emerges after $\alpha = 0.3$. The Mott phase has a reentrance as a function of hopping strength at fixed chemical potential. Beyond $\alpha = 0.3$ (for $K = 2$) curves of the particle and the hole sector intersect at such a large value of the hopping amplitude that the second order perturbation theory fails to capture this region. A final remark about the figure is that, for strong magnetic field, i.e $\alpha_c > 0.3$ the phase diagram takes the shape of the one dimensional case found in Ref.[10]. The re-entrant phase behavior

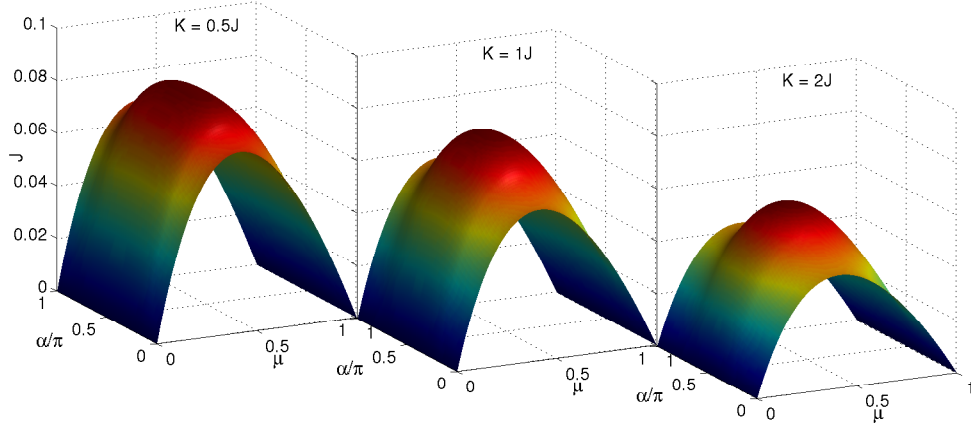


FIG. 5. Mott insulating phase boundary calculated within variational mean field approach as a function of the magnetic field strength and the chemical potential for $K = 0.5J$, $K = 0.5J$, $K = 0.5J$. The region below(above) the plotted surface is the insulating(superfluid) state.

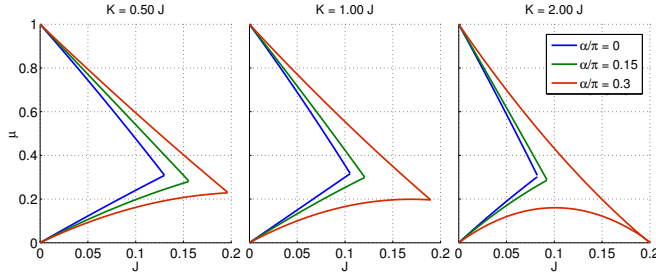


FIG. 6. Phase diagram of the two leg ladder from strong coupling expansion up to the second order for different magnetic fields and inter-leg to intra-leg hopping ratios.

found in one dimensional systems appears with the increase of magnetic field for the two leg ladder. This reentrant behavior was not observed in the results of strong coupling perturbation in one, two or three dimensions, or in two dimensional lattice under a magnetic field (in [13–15] perturbation was carried out up to the third order). Existence of this reentrant phase is also supported by our DMRG results, which is the subject of the next section.

VII. DMRG CALCULATIONS

Density Matrix Renormalization Group (DMRG) theory is proved to provide numerically exact solutions of one dimensional lattice systems[16, 17]. This method has been extensively applied to the Bose Hubbard model[10, 11, 18] and shown to be one of the most reliable approaches for quasi-one dimensional systems. Thus, in this section, we use DMRG to calculate the Mott transition boundary for the two leg Bose Hubbard ladder under a magnetic field.

We use a method similar to [19], namely rung by rung enlargement, but employ single rung enlargement [20] in the construction of superblock Hamiltonian. We use the finite system DMRG algorithm for a ladder of 60 rungs and for each

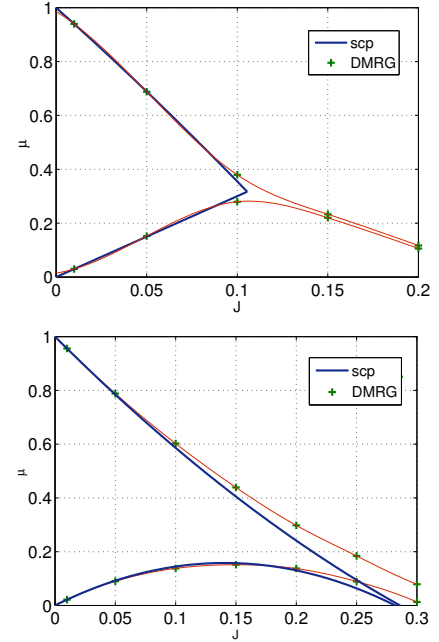


FIG. 7. Phase diagram of the two leg Bose Hubbard ladder from DMRG for $\alpha = 0$ on the left and $\alpha/\pi = 0.45$ on the right. For comparison the strong coupling results are also shown.

site we set the maximum occupancy $n_{max} = 4$. Particle number conservation is used to diagonalize only the $N_{particle} = N_{sites}$ sector of the superblock Hamiltonian or $N_{particle} = N_{sites} \pm 1$ as additional target states. Further details about the projection to the space with different fillings are given in the next section.

Calculation of the Mott phase boundary via DMRG is very similar to the strong coupling perturbation method. One needs energies of the Mott phase together with the additional particle and hole states to find the phase boundary. The energies of particle and hole states are calculated as additional target states in DMRG implementation[10]. In Fig.7, one can see

the good agreement between the strong coupling result and DMRG. For larger values of hopping, the strong coupling deviates from DMRG, as expected for a perturbative method. Another point is that the existence of reentrance is also validated by DMRG results. We show the similar phase for $\alpha = 0.45$ in Fig. (7). It is seen that strong coupling calculations give relatively poor results above $J \approx 0.2$.

Finally, we note that the tip of the Mott insulator region requires a special treatment with DMRG. The two branches coming from particle and hole sector intersect only in the thermodynamic limit, whereas our system is composed of only 60 rungs. There are several approaches (like consideration of the correlation length and extrapolation to Luttinger liquid correlation function in [10]) to remedy this situation. As the critical behavior of the tip is not our main concern in this paper, we do not perform a similar analysis.

VIII. EVIDENCE OF STRONGLY CORRELATED PHASES

In the previous sections, we performed various calculations that can only work close to the Mott insulator phase. Theoretical approaches are limited for 2D Bose Hubbard model under a magnetic field, particularly for strong fields. This is due to the complicated single particle spectrum as well as the interplay between strong correlations and the high number of degeneracies. Both strong coupling and mean field approaches work in the region where such correlations are weak. On the other hand, this is exactly the region where novel phases are expected. For this reason, the characterization of the two dimensional Bose Hubbard model exposed to a strong magnetic field is attracting close attention. There have been several proposals that try to connect these strongly correlated states with the formation of vortex lattice or with the incompressible quantum liquids found in the quantum Hall effects. [5] The absence of an encompassing theoretical model makes it a hard task to identify the physics of this regime.

Both the strong coupling expansion and the mean field theory as discussed in the previous sections use the Mott insulator state as their starting point. As a result, their range of validity is limited to densities close to integer filling. In the other limit, the Gross Pitaevskii approximation assumes a uniform gas spread over the lattice to reveal the dynamics of the system. Compared to these theoretical approaches, DMRG has a very wide range of applicability regardless of the particle number, strength of the field and the interaction. One can calculate the ground state of the system for a finite lattice with any number of particles for all values of the magnetic field and the interaction strength. In this section, we use DMRG method to study the two leg Bose Hubbard Model under magnetic field outside the Mott insulator region, and look for evidence for strongly correlated behavior.

Here, we limit DMRG calculations to hard core bosons in the infinite U limit, providing an easier implementation of the algorithm as the Hilbert space is drastically reduced by excluding multiple occupation of each site. This limit is particularly important for correlated states as the gaps in the spectrum are expected to be more prominent with strong interactions.

Within this constraint, each site is allowed to be empty or have only one boson so that maximum occupation number $n_{max} = 1$ and the terms with the on site interaction in the Hamiltonian becomes only a constraint in the Hilbert space. Bose Hubbard model in this limit can be mapped to spin-XXZ model, where ground state is at half filling. We find that our system has a ground state at half filling not only for $\alpha = 0$ but also for nonzero α . In the two limits; all sites are empty and all sites are filled, ground state energy is zero and minimum of the energy is always at half filling which is in the middle of these two limits.

The energy gap between the ground state and first two excited states is shown in Fig.9 for half filling. From the figure, it can be seen that spectrum of the three lowest lying states changes abruptly to at $\alpha_c/\pi \approx 0.21$. This plot is symmetric around $\alpha/\pi = 0.5$ so we only display the half. The critical value found here is consistent with the one found in single particle solution, which are equal to 0.2148 or 0.7852.

To get the energies at different fillings DMRG code must be restricted to a different particle number conserving subspace. We use the route proposed by Ramanan *et al.*[18] in which the plateaus in the chemical potential versus the density plots and the corresponding compressibilities are obtained successfully. We again have a system length $L = 60$ that has $2 \times L = 120$ sites. Beginning from $L = 4$ and total number of particles $N = 4$, we increase both the lattice length and the number of particles up to where number of particles is $N = 10$. After that, the lattice length is increased while total number of particles held fixed at 10. Whenever the lattice length reaches to $L = 60$, finite system sweeps are used to decrease energy. Next, we increase the total particle number by 1 keeping the system size fixed and perform 5 sweeps to get the energy for this new filling. Repeating this procedure, we get energies where the particle number is increased up to $N = 110$. At the end, energies of systems from $N = 10$ to $N = 110$ particles placed on $2 \times L = 120$ sites are obtained. After that, the gap formula defined by Cooper *et al.*[21]

$$\Delta = N \left[\frac{E(N+1)}{N+1} + \frac{E(N-1)}{N-1} - 2 \frac{E(N)}{N} \right] \quad (27)$$

is used, which minimizes the finite size effects.

We show this gap for various values of magnetic field in Fig.8. It is seen that the gap oscillates between zero and nonzero values for low densities and becomes negative towards integer filling. Apart from that there are three dominant peaks one is always at $1/2$ and the other two depend on α . Magnitude of these changing peaks are also seen to be getting smaller and smaller as the field approaches to $1/2$. It is interesting to compare these peaks by defining the filling factor[22],

$$\nu = \frac{n}{f} \quad (28)$$

where n is particle density and f is vortex density defined as the phase attained around a unit cell divided by 2π which means $f = \alpha/\pi$ in our model. We see that the corresponding distinct values of the filling factors for the peaks in Fig.8

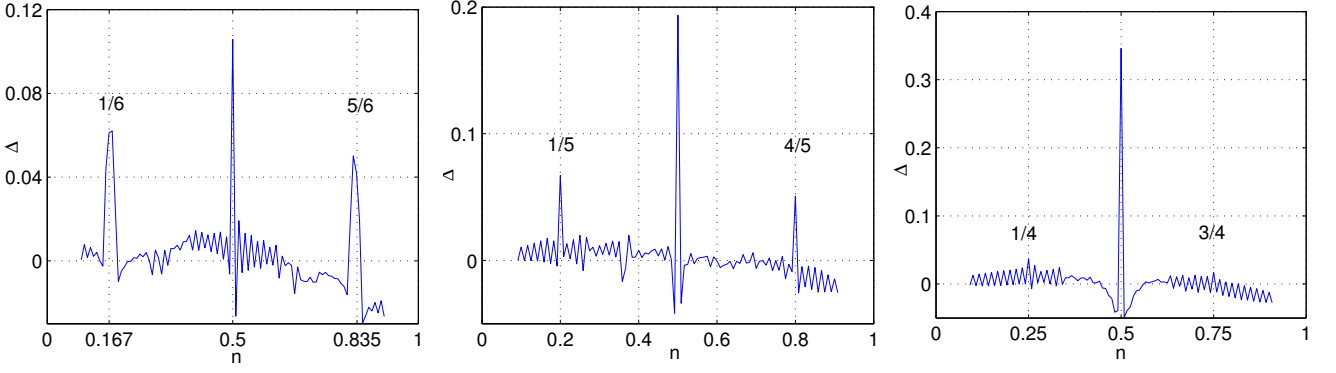


FIG. 8. Particle-hole energy gap defined in Eq.27 as a function of particle density for $\alpha = 1/3$ in the first figure, $2/5$ in the second panel and $1/2$ in the third panel. For each value of α , a different peak is seen in the energy gap where the peaks are symmetric around half filling. Apart from the dominant peaks at $1/6, 5/6$ for $\alpha = 1/3$, $1/5, 4/5$ for $\alpha = 2/5$ and $1/4, 3/4$ for $\alpha = 1/2$ there is a persistent peak at half filling.

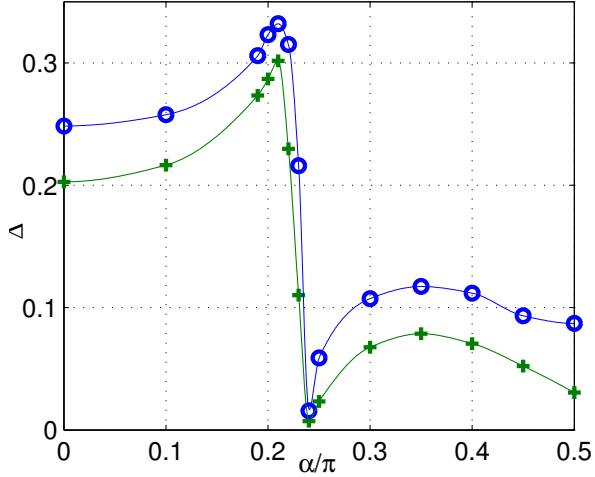


FIG. 9. Gap between ground state and two excited states for different magnetic fields at half filling for hard core interaction. The gap between first excited state $E^1 - E^0$ is shown by green '+', whereas the one for $E^2 - E^0$ is shown by blue 'o'. Thin lines are spline interpolation to data points. Spectrum shows a jump at $\alpha_c/\pi = 0.21$ which is very close to critical magnetic field calculated from the single particle spectrum.

are obtained as $\nu = 1/4, 3/4, 5/4$ for $\alpha/\pi = 1/3$; $\nu = 1/4, 5/8, 1$ for $\alpha/\pi = 2/5$, and $\nu = 1/4, 1/2, 3/4$ for $\alpha/\pi = 1/2$.

The dependence of the gap on the filling fraction is a clear evidence of the role played by the interactions. However our simple finite size DMRG calculations can not reveal the character of correlations within these states. Future studies of the system in this limit must include larger system sizes, finite on-site interactions and a careful consideration of finite size effects to reveal the physics of possible correlated states in the two-leg Bose Hubbard ladder.

IX. CONCLUSION

Our calculations lead to a number of conclusions related to the recent experiment Ref.[7].

The experiment has probed only the limit where the number of particles per site is high, which can mostly be described by the Gross-Pitaevskii level approximations. The reported phase transition between the two phases is driven by the change in the character of the single particle spectrum rather than interactions. In this limit, the effect of interactions is expected to be quantitative rather than qualitative. Our calculations indicate that the interactions will shift the boundary between the Meissner and Vortex phases, however observation of this shift is complicated by the uncertainty due to finite temperature in the experiments. A recent paper [23] argues that another effect of the interactions would be the spontaneous breaking of the symmetry between the two legs. As our calculations have this symmetry built in we cannot investigate such a transition.

While the current experiment operates in the superfluid regime, it is natural to expect further experiments in this system to probe the region with only a few particles per site where the insulating state is likely. We expect our strong coupling and DMRG results to be quantitatively correct for the Mott transition boundary. While the effect of the external confining potential is weak in the experiment, a wedding cake structure would be a clear indication of the Mott transition. Such a wedding cake structure can be observed by not only looking at the density but can also be deduced from the link currents investigated by the method used in the present experiment.

Finally, our DMRG results for non-integer filling factors provide some evidence for the possibility of correlated phases in this system. However we can not confidently assert the presence of these phases due to the finite size limitations of our calculation. To judge the viability of the experimental observation of these phases a better characterization of their gaps and correlation properties must be made. Nonetheless our results indicate that this regime should be interesting to investigate experimentally.

In conclusion, we worked on the two leg Bose Hubbard

ladder exposed to magnetic field within various theoretical approaches and implemented DMRG to study the behavior of the system. We found that the system has two distinctively different regimes in agreement with the recent experiment. The shape of the Mott insulator region is obtained with three different methods; variational mean field theory, strong coupling perturbation theory and DMRG. We found that the shape of the lobe is consistent within DMRG and strong coupling approximation while the results of the mean field theory is relatively poor. Apart from the determination of the Mott lobes, system is found to display novel physical properties as a result of the single particle spectrum. We believe that this model serves as an important tool for understanding the general properties of the optical lattices coupled to a gauge field. In the final part of the paper, we calculated the excitation gap

for non-integer filling and found distinct peaks at simple fractions of particle number to flux quanta. This regime will be investigated further in subsequent work.

ACKNOWLEDGMENTS

While this manuscript was in preparation, the same system has been investigated theoretically in [24] and [25]. We believe our results and these theoretical papers are complementary to each other. M.Ö.O. is supported by TUBITAK grant 112T974. A.K. thanks Levent Subaşı and Onur Umucalılar for many useful discussions, and Tomotoshi Nishino and Andrej Gendiar for useful correspondence on DMRG.

-
- [1] Y.-J. Lin, R.L. Compton, K. Jimenez-Garcia, J.V. Porto, and I.B. Spielman, *Nature* **462**, 628-632 (2009)
 - [2] H. Miyake, G.A. Siviloglou, C.J. Kennedy, W.C. Burton, and W. Ketterle, *Phys. Rev. Lett.* **111**, 185302(2013)
 - [3] M. Aidelsburger, M. Atala, M. Lohse, J.T. Barreiro, B. Paredes, and I. Bloch, *Phys. Rev. Lett.* **111**, 185301 (2013)
 - [4] D.R. Hofstadter, *Phys. Rev. B* **14**, 2239 (1976)
 - [5] G. Möller and N.R. Cooper, *Phys. Rev. Lett.* **103**, 105303 (2009); N.R. Cooper and J. Dalibard, *Phys. Rev. Lett.* **110**, 185301 (2013)
 - [6] R. O. Umucalılar and M. O. Oktel, *Physical Review A* **76**, 055601 (2007).
 - [7] M. Atala, M. Aidelsburger, M. Lohse, J.T. Barreiro, B. Paredes, and I. Bloch, *Nature Physics* **10**, 588-593 (2014)
 - [8] Ahmet Keles. *Rotating Two Leg Bose Hubbard Ladder*. Master Thesis, Bilkent University, 2009. <http://www.thesis.bilkent.edu.tr/0003932.pdf>
 - [9] L. D. Landau and E. M. Lifshitz. *Statistical physics: Vol.2*. Pergamon Press, 1980.
 - [10] T.D. Kuhner, S.R. White, and H. Monien. *Physical Review B* **61**, 12474, (2000).
 - [11] T.D. Kuhner and H. Monien, *Physical Review B* **58**, R14741 (1998).
 - [12] M.P.A. Fisher, P.B. Weichman, G. Grinstein, and D.S. Fisher. *Phys. Rev. B* **40**, 546 (1989).
 - [13] J.K. Freericks and H. Monien. *Europhysics Letters* **26**, 545 (1994).
 - [14] J.K. Freericks and H. Monien. *Phys. Rev. B* **53**, 2691 (1996).
 - [15] M. Niemeier, J.K. Freericks, and H. Monien, *Phys. Rev. B* **60**, 2357 (1999)
 - [16] S.R. White, *Phys. Rev. Lett.* **69**, 2863 (1992)
 - [17] S.R. White, *Phys. Rev. B* **48**, 10345 (1993).
 - [18] S. Ramanan, T. Mishra, M.S. Luthra, R.V. Pai, and B.P. Das. *Phys. Rev. A*, **79**, 013625 (2009).
 - [19] Meetu Sethi Luthra, Tapan Mishra, Ramesh V. Pai, and B. P. Das. *Physical Review B*, **78** (165104), (2008).
 - [20] S.R. White, *Phys. Rev. B*, **72**, 180403(R), 2005.
 - [21] N. R. Cooper, N. K. Wilkin, and J. M. F. Gunn. *Phys. Rev. Lett.* **87**, 120405 (2001).
 - [22] N. R. Cooper. *Advances In Physics*, **57** (6) 539–616, 2008.
 - [23] R. Wei and E.J. Mueller, *Phys. Rev. A*, **89**, 063617 (2014)
 - [24] M. Piraud, F. Heidrich-Meisner, I.P. McCulloch, S. Greschner, T. Vekua, and U. Schollwöck, *arXiv preprint arXiv:1409.7016*, 2014
 - [25] D. Hülge and B. Paredes, *Phys. Rev. A* **89**, 023619 (2014)